

Iron(IV)–Imido Complexes

Comparison of the Reactivity of Nonheme Iron(IV)–Oxo versus Iron(IV)–Imido Complexes: Which is the Better Oxidant?*

Anil Kumar Vardhaman, Prasenjit Barman, Suresh Kumar, Chivukula V. Sastri,*
Devesh Kumar,* and Sam P. de Visser*

High-valent heme and nonheme iron(IV)–oxo complexes play key roles in biology as catalytic intermediates in enzymes, where they catalyze vital biotransformations for human health, including detoxification processes in the liver and also the biosynthesis of hormones.^[1,2] Mono- and dioxygenases bind and utilize molecular oxygen on an iron center and form a catalytically active iron(IV)–oxo species that transfers the oxygen atom to substrate. Technically, using a nitrogen donor one should be able to synthesize the analogous iron(IV)–imido and/or iron(V)–nitrido complexes. Although these complexes are rare in nature, evidence exists of substrate aziridination by cytochrome P450 enzymes that presumably takes place by a high-valent iron(IV)–nitrido or –imido complex.^[3] Several iron–porphyrin models with nitrene or imido ligands have been synthesized and their reactivity patterns implicated efficient aziridination of olefins.^[4,5]

By contrast to iron(IV)–oxo complexes, which have been extensively studied over the years, only few studies have been reported on its closely related iron(V)–nitrido species ($\text{Fe}^{\text{V}}\equiv\text{N}$) or the iron(IV)–imido ($\text{Fe}^{\text{IV}}=\text{NR}$) species. In principle, these high-valent metal–nitrido/imido complexes should have strong oxidative power and capable to catalyze isolobal amination reactions. During the past decade, the chemistry of metal-catalyzed aziridination of alkenes and aminidation of aliphatic C–H bonds using iminodane reagents have been

studied by several groups.^[6,7] In recent years, the putative metal–nitrogen multiple-bonded species have been isolated and spectroscopically characterized, which led to significant progress on the understanding of its fundamental chemical properties.^[6,8] However, details on its potential as nitrogen atom transfer agent are lacking and little knowledge exists in its relative reactivity with respect to the well-known iron(IV)–oxo species.^[8b]

In nonheme iron chemistry, the aromatic amination of ligands by an iron–nitrido complex was reported by several groups,^[6c,9] and recently, the spectroscopic characterization of the iron(IV)–tosylimido (tosylimido²⁻ = NTs) complex with pentadentate N4Py ligand (N4Py = *N,N*-bis(2-pyridylmethyl)-*N*-bis(2-pyridyl)methylamine), $[\text{Fe}^{\text{IV}}(\text{NTs})(\text{N4Py})]^{2+}$, was described (Figure 1).^[10] As this species was

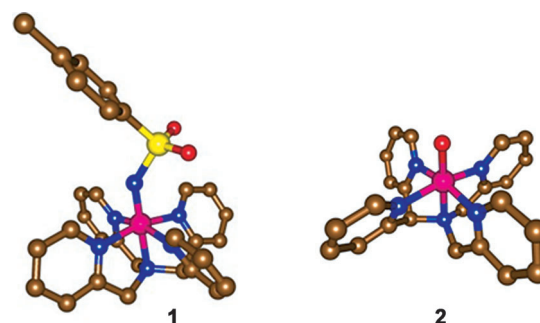


Figure 1. Structures of $[\text{Fe}^{\text{IV}}(\text{NTs})(\text{N4Py})]^{2+}$ (**1**) and $[\text{Fe}^{\text{IV}}(\text{O})(\text{N4Py})]^{2+}$ (**2**) derived from computational and crystallographic results. Hydrogen atoms are omitted for clarity. Fe magenta, C brown, O red, N blue, S yellow.

shown to have a relatively long lifetime, it makes it highly suitable for reactivity studies, especially since the iron(IV)–oxo analogue can be studied in tandem. We therefore took the opportunity to pursue a comparative reactivity study of $[\text{Fe}^{\text{IV}}(\text{NTs})(\text{N4Py})]^{2+}$ (**1**) and $[\text{Fe}^{\text{IV}}(\text{O})(\text{N4Py})]^{2+}$ (**2**) with substrates.

Complexes **1** and **2** were generated in an acetonitrile solution in situ using either PhINTs as tosylimido donor or PhIO as oxygen atom donor using procedures reported before.^[10,11] The identity of complex **1** was confirmed on the basis of visible features with an intense LMCT band at 445 nm ($\epsilon = 2700 \text{ L mol}^{-1} \text{ cm}^{-1}$) and a low energy 660 nm band ($\epsilon = 250 \text{ L mol}^{-1} \text{ cm}^{-1}$) that arises from ligand field transitions characteristic for $S=1$ iron(IV) complexes (Supporting Information, Figure S2). The electron spray ionization mass spectrum (Supporting Information, Figure S3) gave a major

[*] A. K. Vardhaman, P. Barman, Dr. C. V. Sastri
Department of Chemistry
Indian Institute of Technology Guwahati
Assam, 781039 (India)
E-mail: sastricv@iitg.ernet.in

S. Kumar, Dr. D. Kumar
Department of Applied Physics
Babasaheb Bhimrao Ambedkar University
School for Physical Sciences
Vidya Vihar, Rae Bareilly Road, Lucknow (UP), 226025 (India)
E-mail: dkclcre@yahoo.com

Dr. S. P. de Visser
Manchester Institute of Biotechnology and School of Chemical
Engineering and Analytical Science, The University of Manchester
131 Princess Street, Manchester M1 7DN (United Kingdom)
E-mail: sam.devisser@manchester.ac.uk

[**] Research support was provided by the Department of Science and Technology, India (SR/S1/IC-02/2009) and Council for Scientific & Industrial Research (01(2527)/11/EMR-II) to C.V.S. The National Service of Computational Chemistry Software (NSCCS) is acknowledged for CPU time. D.K. acknowledges Department of Science and Technology (New Delhi) for a Ramanujan Fellowship.

Supporting information for this article is available on the WWW under <http://dx.doi.org/10.1002/anie.201305370>.

peak at $m/z = 741.0751$ corresponding to $[\text{Fe}^{\text{IV}}(\text{NTs})(\text{N4Py})\text{-(OTf)}]^+$ with an isotope pattern that matches the theoretically expected distribution. Thioanisole was added to the solution of **1** at 273 K, which led to the decay of the characteristic peak at 660 nm in the UV/Vis spectrum concomitant with the appearance of its iron(II) precursor ($\lambda_{\text{max}} = 450$ nm) with an isosbestic point at 516 nm (Supporting Information, Figure S4). Aminidation of thioanisole to *N*-*p*-tosylmethylphenyl sulfilimine was obtained in about 85 % yield,^[12] and a second-order rate constant for this reaction was evaluated of $0.260 \text{ L mol}^{-1} \text{ s}^{-1}$ (Supporting Information, Table S5). In contrast, the second-order rate constant for **2** determined under the same reaction conditions was found to be only $0.050 \text{ L mol}^{-1} \text{ s}^{-1}$ (Figure 2a; Supporting Information, Table S6). It appears, therefore, that the $[\text{Fe}^{\text{IV}}(\text{NTs})(\text{N4Py})]^{2+}$ complex reacts with thioanisole with rate constants that are about five times higher than those found for the $[\text{Fe}^{\text{IV}}(\text{O})(\text{N4Py})]^{2+}$ complex.

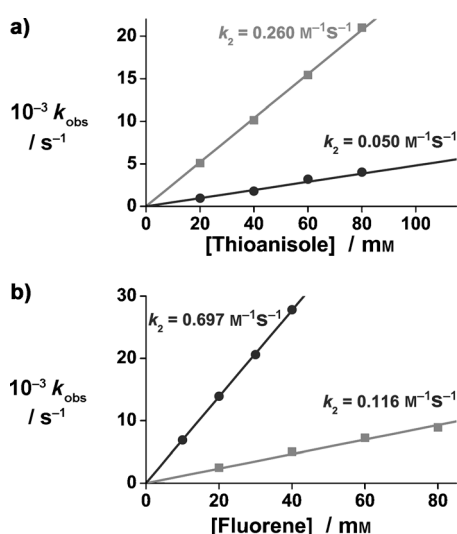


Figure 2. Second-order rate constants determined in the reactions of 1 mM $[\text{Fe}^{\text{IV}}(\text{NTs})(\text{N4Py})]^{2+}$ **1** (■) and $[\text{Fe}^{\text{IV}}(\text{O})(\text{N4Py})]^{2+}$ **2** (●) in CH_3CN solution against various concentrations of a) thioanisole at 273 K and b) fluorene at 298 K.

The pseudo first-order rate constants were then determined for the reaction of **1** and **2** with various *p*-substituted thioanisoles (Supporting Information, Table S7). From a direct comparison of the k_{obs} values for the reactions of **1** and **2** with different *para*-substituted thioanisoles, it is evident that the reactivity of **1** is more sensitive than that of **2** to substitution at the *para* position of the substrate. In fact, the difference in reactivity between **1** and **2** increased when electron-donating groups at the *para* position were employed; for instance, in the reaction with *p*-methoxythioanisole the difference in reactivity was found to be more than 50 times. We then created Hammett plots, for a quantitative examination of the substituent effect on the reaction rates. For **2**, a linear correlation with σ was found with a $\rho = -0.90$. In contrast, when a similar plot was made for **1**, non-linearity was observed with $\rho = -3.36$ (Supporting Information, Figure S8),

which is likely as a result of additional stabilization of positive charge in the transition state by electron-donating groups in the *para* position of thioanisole and thus enhanced the overall rate of oxidation, as also will be discussed in the computational section. To accommodate the additional stabilization of the positive charge in the transition state, new Hammett plots were now made using σ^+ values leading to ρ values of -1.92 and -0.52 , respectively, for **1** and **2** (Supporting Information, Figure S9). This difference in slopes quantitatively reflect that **1** is more sensitive to electronic effects of the *para* substituents than **2**. Further, the plot of $\log(k_X/k_H)$ values against the E^0_{ox} of sulfides gave a linear correlation with a slope of -7.1 and -1.92 for **1** and **2**, respectively (Supporting Information, Figure S10). Such a large negative slope obtained from these plots implicates a rate determining electron transfer from sulfides to **1** rather than a group transfer.^[13]

Considering the high reactivity of **1** over **2** in the oxidation of thioanisole, we then evaluated the hydrogen atom transfer (HAT) capability of **1**. It has been shown that the rate constant of HAT reactions often correlates with the strength of the C–H bond that is broken, that is, $\text{BDE}_{\text{C-H}}$ or bond dissociation energy,^[14] we therefore studied the rates of HAT between **1** and substrates with a range of $\text{BDE}_{\text{C-H}}$ values: xanthene, 9,10-dihydroanthracene (DHA), 1,4-cyclohexadiene (CHD), fluorene, and triphenylmethane. Indeed a plot of the logarithm of the rate constant of HAT by **1** versus the $\text{BDE}_{\text{C-H}}$ value of the substrate gives a linear correlation, Figure 3, (Supporting Information, Table S11,

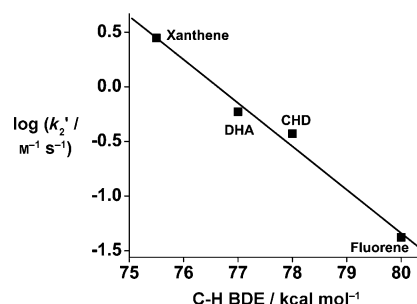


Figure 3. Correlation of the second-order rate constants (determined at 288 K) for HAT by **1** with $\text{BDE}_{\text{C-H}}$ of substrates.

Figure S12). However, when excess triphenylmethane ($\text{BDE}_{\text{C-H}} = 81 \text{ kcal mol}^{-1}$) was added to a solution of **1** at 298 K, no change in 660 nm absorption band was observed, despite observable reactivity with fluorene, which has a comparable $\text{BDE}_{\text{C-H}}$.^[11] Most probably the difference in reactivity between these two substrates with closely related $\text{BDE}_{\text{C-H}}$ values is due to stereochemical clashes of **1** with the approaching substrate. This is particularly important for substrates with bulky groups adjacent to the hydrogen abstraction center, such as triphenylmethane.

Subsequently, we compared the relative activity in HAT processes of **1** and **2** using fluorene as the substrate (Supporting Information, Table S13). The reaction of **1** and **2** follows pseudo first-order kinetics, and second-order rate constants were determined for each system (Figure 2b;

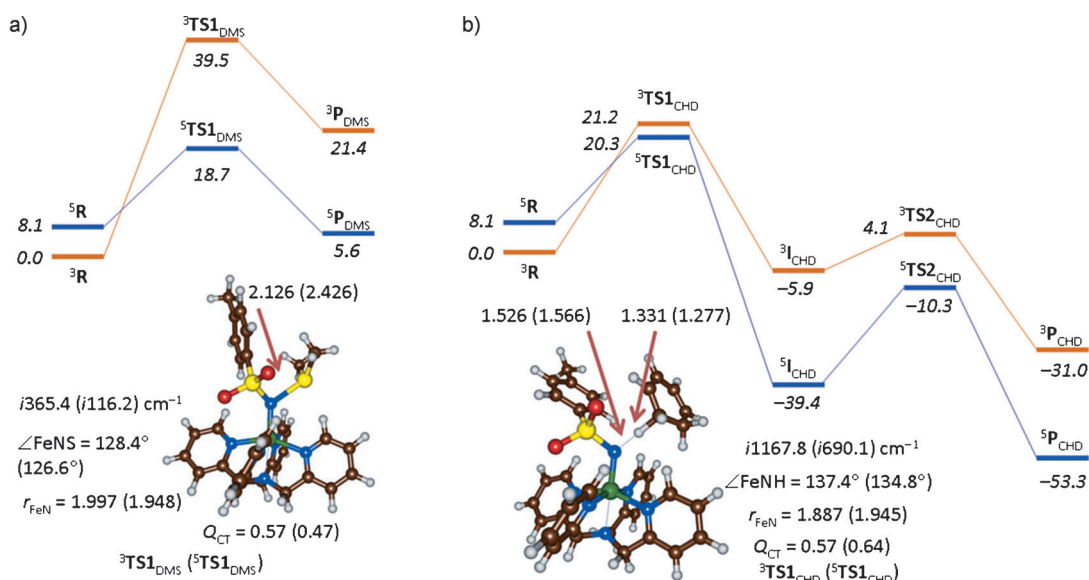


Figure 4. DFT calculated potential-energy landscapes for DMS sulfoxidation and hydrogen atom abstraction from CHD by $[\text{Fe}^{\text{IV}}(\text{NTs})(\text{N4Py})]^{2+}$. Energies are ΔG^\ddagger in kcal mol^{-1} relative to a reactant complex with solvent and dispersion energy corrections included. Also given are optimized geometries of the transition states with bond lengths [Å], the degree of charge transfer (Q_{CT}), and the imaginary frequency in the TS [cm^{-1}].

Supporting Information, Table S6). At 298 K, complex **1** decayed with a second order rate constant of $0.116 \text{ L mol}^{-1} \text{ s}^{-1}$ to form 9*H*,9'*H*-[9,9']bifluorenyl (9,9'-bifluorene) products in about 32% yield. These results indicate that **1** effectively acts as a one-electron oxidizing agent in HAT reactions, whereby the 32% yield of 9,9'-bifluorene reflects the conversion of about 64% of iron(IV)-imido complex in two one-electron oxidation steps of fluorene. By comparison, complex **2** decays with a $k_2 = 0.697 \text{ L mol}^{-1} \text{ s}^{-1}$ to form fluorenone as the dominant product.^[15] The observed slower rate (ca. 6 times) of **1** relative to **2** for C–H bond activation is opposite to that observed for thioanisole oxidation (see above). This observation indicates that iron(IV)-tosylimido complex is a less-effective oxidant than iron(IV)-oxo for hydrogen atom abstraction reactions. Indeed, recent computational studies on nonheme iron(IV)-oxo versus iron(IV)-nitrido complexes gave higher hydrogen atom abstraction barriers from methane for the latter system, in agreement with our results herein.^[16]

Further evidence of a rate-determining HAT reaction comes from kinetic isotope effect (KIE) studies of **2** with fluorene (KIE = 30). Such large KIE values exceed the semi-classical limit and suggest strong tunneling behavior in the reaction mechanism. On the other hand, the reaction of deuterated fluorene with **1** gave a KIE of only 7, although it is still regarded as a HAT mechanism (Supporting Information, Figures S14, S15).

To gain insight into the details of the reaction mechanisms of substrate activation by iron(IV)-tosylimido complexes, we decided to do an additional density functional theory study and compare the work with the experimental work reported above and earlier computational studies on the reactivity of **2** with substrates.^[17] We calculated the reaction mechanisms of **1** with dimethylsulfide (DMS) and CHD as model substrates for sulfoxidation and HAT reactions. Dehydrogenation of

CHD is a stepwise process with two sequential hydrogen-atom abstraction barriers TS1_{CHD} and TS2_{CHD} by a radical intermediate I_{CHD} leading to benzene products P_{CHD} . Figure 4 displays the calculated free energy landscapes and the rate-determining transition states (TS1) for the two reactions on the lowest lying triplet and quintet spin-state surfaces. Similar to previous studies, we find a concerted one-step mechanism via a transition state TS1_{DMS} for substrate sulfoxidation by both **2** and **1**, leading to products P_{DMS} .^[18] Despite the fact that substrate sulfoxidation by either **1** or **2** appears to be concerted through a single rate-determining transition state, actually there are some critical differences between the two sulfoxidation processes that lead to changes in the Hammett plots for **1** versus **2**. In case of **1**, the analysis of the orbital occupation and group spin densities and charges of $^3,^5\text{TS1}_{\text{DMS}}$ shows that in the sulfoxidation transition states a large amount of charge transfer has taken place from substrate to oxidant; $Q_{\text{CT}} = 0.57$ (0.47) for $^3\text{TS1}_{\text{DMS}}$ ($^5\text{TS1}_{\text{DMS}}$), respectively. Furthermore, the orbital occupations and group spin densities (Supporting Information, Tables S18, S31) implicate a product-like electronic configuration. In contrast, the electron-transfer processes from substrate to iron(IV)-oxo happen at a much later timescale and give group spin densities much more in line with the reactant structure.^[18] To find the origin of these differences in reactivity we calculated the electron affinities of **1** and **2**, which gave values of $\Delta E + \text{ZPE} + E_{\text{solv}} = 120.5$ and $94.6 \text{ kcal mol}^{-1}$, respectively. Therefore, **1** is more electrophilic than **2**.

The substrate sulfoxidation mechanism by $[\text{Fe}^{\text{IV}}(\text{NTs})(\text{N4Py})]^{2+}$ shows analogy to aromatic hydroxylation by **2**, where also a large energy difference between $^3\text{TS1}$ and $^5\text{TS1}$ was calculated.^[17b] However, there are critical differences and one relates to the orientation of the substrate. Thus, on the quintet spin-state surface the substrate usually attacks from the top and aligns itself along the Fe–O/N bond owing to

electron transfer into the $\sigma^*_{z^2}$ orbital.^[17,19] In $[\text{Fe}^{\text{IV}}(\text{NTs})-(\text{N4Py})]^{2+}$ this alignment is not possible because of stereochemical constraints of the NTs group with the approaching substrate and thus a more sideways approach is essential. As a consequence, the quintet spin barriers have increased in energy and in the case of HAT from CHD $^5\text{TS1}_{\text{CHD}}$ is competitive with $^3\text{TS1}_{\text{CHD}}$. These studies support the experimental observation mentioned above that **2** will be better in catalyzing HAT reaction mechanisms owing to lesser stereochemical interactions between substrate and oxidant as compared to **1**. Furthermore, the stereochemical interactions between oxidant and the approaching substrate destabilize the transition states and increase the HAT process for **1**. This effect is larger for HAT processes by **1** than by **2** as the (almost) linearity of the Fe–O–H angle in the quintet spin state will ensure large distances between the rest of the substrate and the oxidant. Approach under an angle of 120° as in **1**, however, brings the substrate closer to the equatorial ligand of the oxidant and hence stereochemical repulsions are larger and barriers are raised. As a consequence, the HAT barriers for **1** are above those for **2** in support of the experimental rate constants in Figure 2.

The dehydrogenation reaction has low barriers TS1_{CHD} on the triplet and quintet spin states, leading to a radical intermediate. However, the subsequent dehydrogenation of hydrogen atom abstraction via **TS2** encounters significantly larger barriers of well over $\Delta G + E_{\text{solv}} > 25 \text{ kcal mol}^{-1}$, and consequently will be difficult. Instead theory predicts that the radical will dissipate from the reaction center rather than donating a second hydrogen atom to the oxidant. A subsequent collision of two of these radicals will then form a dimer at much lower energetic costs than dehydrogenation products, which is indeed what was observed experimentally. The fact that these dimers are not formed in the reaction of **1** with triphenylmethane may be due to stereochemical restrictions in dimer formation. The large **TS2** barrier obtained for the reaction of **1** with CHD contrasts that found for the reaction of **2** with CHD, where typically barriers of less than 5 kcal mol^{-1} are obtained.^[20] This change in **TS2** barrier leads to fundamental differences in substrate activation and consequently product distributions.

So what is the origin of the differences in reactivity of **1** over **2** and why is sulfoxidation preferred for **1**, whereas hydrogen atom abstraction is favored by **2**? Hydrogen atom abstraction is accompanied by the breaking of the C–H bond of the substrate and the formation of an O/N–H bond with the oxidant. It has been shown that hydrogen atom abstraction barriers tend to correlate with the $\text{BDE}_{\text{C-H}}$ bond of the substrate as well as the $\text{BDE}_{\text{O-H}}$ bond of the oxidant.^[14,21] We calculated values of $\text{BDE}_{\text{N-H}} = 94.4 \text{ kcal mol}^{-1}$ and $\text{BDE}_{\text{O-H}} = 96.7 \text{ kcal mol}^{-1}$ for **1** and **2**, respectively, which implies that **2** and **1** should be similarly good oxidants of HAT reactions. Instead, differences in HAT catalysis are most likely originated by stereochemical repulsions of the approaching substrate with the oxidant. Thus, as shown in Figure 4, during HAT the substrate attacks the NTs group under an angle Fe–N–H of 137.4° (134.8°) for $^3\text{TS}_{\text{CHD}}$ ($^5\text{TS}_{\text{CHD}}$), respectively, whereas in $[\text{Fe}^{\text{IV}}(\text{O})(\text{N4Py})]^{2+}$ the approach will be along the Fe–O axis in the quintet spin state.^[22] Consequently,

the attack of substrate on **1** will be more stereochemically constraint than in **2** and thus generally higher barriers for HAT reactions.

In summary, we present herein the first comparative study on the reactivity patterns of nonheme iron(IV)–oxo versus iron(IV)–imido. We show that owing to the larger electron affinity of the oxidant iron(IV)–imido is a better oxidant of sulfoxidation reactions than iron(IV)–oxo. By contrast, these trends are reversed for stepwise one-electron transfer reactions, such as hydrogen atom abstraction reactions where stereochemical interactions upon substrate approach determine the relative rate constants.

Experimental Section

Detailed procedures and methods of the experiments and computations, which follow those of our previous studies in the field,^[23] are given in detail in the Supporting Information.

Received: June 21, 2013

Revised: August 12, 2013

Published online: September 25, 2013

Keywords: C–H activation · enzyme models · imido ligands · iron · sulfoxidation

- a) M. Sono, M. P. Roach, E. D. Coulter, J. H. Dawson, *Chem. Rev.* **1996**, 96, 2841–2888; b) J. T. Groves, *Proc. Natl. Acad. Sci. USA* **2003**, 100, 3569–3574; c) *Cytochrome P450: Structure, Mechanism and Biochemistry*, 3rd ed. (Ed.: P. R. Ortiz de Montellano), Kluwer Academic/Plenum Publishers, New York, **2004**; d) *Handbook of Porphyrin Science* (Eds.: K. M. Kadish, K. M. Smith, R. Guilard), World Scientific Publishing Co., New Jersey, **2010**; e) *Iron-containing enzymes: Versatile catalysts of hydroxylation reactions in nature* (Eds.: S. P. de Visser, D. Kumar), RSC Publishing, Cambridge, **2011**.
- a) M. Costas, M. P. Mehn, M. P. Jensen, L. Que, Jr., *Chem. Rev.* **2004**, 104, 939–986; b) S. V. Kryatov, E. V. Rybak-Akimova, S. Schindler, *Chem. Rev.* **2005**, 105, 2175–2226; c) M. M. Abu-Omar, A. Loaiza, N. Hontzeas, *Chem. Rev.* **2005**, 105, 2227–2252; d) R. van Eldik, *Coord. Chem. Rev.* **2007**, 251, 1649–1662; e) P. C. A. Bruijninx, G. van Koten, R. J. M. Klein Gebbink, *Chem. Soc. Rev.* **2008**, 37, 2716–2744; f) A. R. McDonald, L. Que, Jr., *Coord. Chem. Rev.* **2013**, 257, 414–428.
- a) R. E. White, M. B. McCarthy, *J. Am. Chem. Soc.* **1984**, 106, 4922–4926; b) E. W. Svaitsits, J. H. Dawson, R. Breslow, S. H. Gellman, *J. Am. Chem. Soc.* **1985**, 107, 6427–6428; c) J. Hohenberger, K. Ray, K. Meyer, *Nat. Commun.* **2012**, 3, 1–13.
- a) D. Mansuy, P. Battioni, J.-P. Mahy, *J. Am. Chem. Soc.* **1982**, 104, 4487–4489; b) J.-P. Mahy, P. Battioni, D. Mansuy, J. Fisher, R. Weiss, J. Mispelter, I. Morgenstern-Badarau, P. Gans, *J. Am. Chem. Soc.* **1984**, 106, 1699–1706; c) J.-P. Mahy, P. Battioni, D. Mansuy, *J. Am. Chem. Soc.* **1986**, 108, 1079–1080.
- a) C.-M. Che, C.-Y. Zhou, E. L.-M. Wong, *Top. Organomet. Chem.* **2011**, 33, 111–138; b) T. W.-S. Chow, G.-Q. Chen, Y. Liu, C.-Y. Zhou, C.-M. Che, *Pure Appl. Chem.* **2012**, 84, 1685–1704.
- a) J. F. Berry, E. Bill, E. Bothe, S. DeBeer George, B. Mienert, F. Neese, K. Wieghardt, *Science* **2006**, 312, 1937–1941; b) P. Comba, C. Lang, C. Lopez de Laorden, A. Muruganatham, G. Rajaraman, H. Wadepohl, M. Zajackowski, *Chem. Eur. J.* **2008**, 14, 5313–5328; c) K. L. Klotz, L. M. Slominski, M. E. Riemer, J. A. Phillips, J. A. Halfen, *Inorg. Chem.* **2009**, 48, 801–803; d) J. J. Scepaniak, J. A. Young, R. P. Bontchev, J. M. Smith,

- Angew. Chem.* **2009**, *121*, 3204–3206; *Angew. Chem. Int. Ed.* **2009**, *48*, 3158–3160; e) P. Leeladee, G. N. L. Jameson, M. A. Siegler, D. Kumar, S. P. de Visser, D. P. Goldberg, *Inorg. Chem.* **2013**, *52*, 4668–4682.
- [7] a) M. J. Zdilla, M. M. Abu-Omar, *J. Am. Chem. Soc.* **2006**, *128*, 16971–16979; b) S. Kundu, E. Miceli, E. Farquhar, F. F. Pfaff, U. Kuhlmann, P. Hildebrandt, B. Braun, C. Greco, K. Ray, *J. Am. Chem. Soc.* **2012**, *134*, 14710–14713; c) J. W. W. Chang, P. W. H. Chan, *Angew. Chem.* **2008**, *120*, 1154–1156; *Angew. Chem. Int. Ed.* **2008**, *47*, 1138–1140.
- [8] a) T. Petrenko, S. DeBeer George, N. Aliaga-Alcalde, E. Bill, B. Mienert, Y. Xiao, Y. S. Guo, W. Sturhahn, S. P. Cramer, K. Wieghardt, F. Neese, *J. Am. Chem. Soc.* **2007**, *129*, 11053–11060; b) R. E. Cowley, N. A. Eckert, S. Vaddadi, T. M. Figg, T. R. Cundari, P. L. Holland, *J. Am. Chem. Soc.* **2011**, *133*, 9796–9811; c) M. P. Mehn, J. C. Peters, *J. Inorg. Biochem.* **2006**, *100*, 634–643; d) C. M. Thomas, N. P. Mankad, J. C. Peters, *J. Am. Chem. Soc.* **2006**, *128*, 4956–4957; e) I. Nieto, F. Ding, R. P. Bontchev, H. Wang, J. M. Smith, *J. Am. Chem. Soc.* **2008**, *130*, 2716–2717; f) E. R. King, E. T. Hennessy, T. A. Betley, *J. Am. Chem. Soc.* **2011**, *133*, 4917–4923; g) Y. Liu, X. Guan, E. L. M. Wong, P. Liu, J. S. Huang, C.-M. Che, *J. Am. Chem. Soc.* **2013**, *135*, 7194–7204; h) E. T. Hennessy, T. A. Betley, *Science* **2013**, *340*, 591–595.
- [9] a) M. P. Jensen, M. P. Mehn, L. Que, Jr., *Angew. Chem.* **2003**, *115*, 4493–4496; *Angew. Chem. Int. Ed.* **2003**, *42*, 4357–4360; b) H. S. Soo, M. T. Sougrati, F. Grandjean, G. J. Long, C. J. Chang, *Inorg. Chim. Acta* **2011**, *369*, 82–91.
- [10] E. J. Klinker, T. A. Jackson, M. P. Jensen, A. Stubna, G. Juhász, E. L. Bominaar, E. Münck, L. Que, Jr., *Angew. Chem.* **2006**, *118*, 7554–7557; *Angew. Chem. Int. Ed.* **2006**, *45*, 7394–7397.
- [11] J. Kaizer, E. J. Klinker, N. Y. Oh, J.-U. Rohde, W. J. Song, A. Stubna, J. Kim, E. Münck, W. Nam, L. Que, Jr., *J. Am. Chem. Soc.* **2004**, *126*, 472–473.
- [12] Small amounts (<15%) of methylphenylsulfoxide products were detected that are likely to be due to hydrolysis of sulfilimine.
- [13] a) Y. Goto, T. Matsui, S.-I. Ozaki, Y. Watanabe, S. Fukuzumi, *J. Am. Chem. Soc.* **1999**, *121*, 9497–9502; b) J. Park, Y. Morimoto, Y.-M. Lee, W. Nam, S. Fukuzumi, *J. Am. Chem. Soc.* **2011**, *133*, 5236–5239.
- [14] a) L. E. Friedrich, *J. Org. Chem.* **1983**, *48*, 3851–3852; b) F. G. Bordwell, J.-P. Cheng, *J. Am. Chem. Soc.* **1991**, *113*, 1736–1743; c) C. V. Sastri, J. Lee, K. Oh, Y. J. Lee, J. Lee, T. A. Jackson, K. Ray, H. Hirao, W. Shin, J. A. Halfen, J. Kim, L. Que, Jr., S. Shaik, W. Nam, *Proc. Natl. Acad. Sci. USA* **2007**, *104*, 19181–19186; d) J. J. Warren, T. A. Tronic, J. M. Mayer, *Chem. Rev.* **2010**, *110*, 6961–7001; e) K. A. Prokop, S. P. de Visser, D. P. Goldberg, *Angew. Chem.* **2010**, *122*, 5217–5221; *Angew. Chem. Int. Ed.* **2010**, *49*, 5091–5095.
- [15] J. R. Bryant, J. M. Mayer, *J. Am. Chem. Soc.* **2003**, *125*, 10351–10361.
- [16] H. Tang, J. Guan, H. Liu, X. Huang, *Inorg. Chem.* **2013**, *52*, 2684–2696.
- [17] a) H. Hirao, D. Kumar, L. Que, Jr., S. Shaik, *J. Am. Chem. Soc.* **2006**, *128*, 8590–8606; b) S. P. de Visser, K. Oh, A.-R. Han, W. Nam, *Inorg. Chem.* **2007**, *46*, 4632–4641; c) S. P. de Visser, *J. Am. Chem. Soc.* **2010**, *132*, 1087–1097.
- [18] a) S. Aluri, S. P. de Visser, *J. Am. Chem. Soc.* **2007**, *129*, 14846–14847; b) D. Kumar, S. P. de Visser, P. K. Sharma, H. Hirao, S. Shaik, *Biochemistry* **2005**, *44*, 8148–8158; c) D. Kumar, G. N. Sastry, S. P. de Visser, *Chem. Eur. J.* **2011**, *17*, 6196–6205.
- [19] a) S. P. de Visser, *J. Am. Chem. Soc.* **2006**, *128*, 15809–15818; b) C. Y. Geng, S. F. Ye, F. Neese, *Angew. Chem.* **2010**, *122*, 5853–5856; *Angew. Chem. Int. Ed.* **2010**, *49*, 5717–5720; c) S. Sahu, L. R. Widger, M. G. Quesne, S. P. de Visser, H. Matsumura, P. Moënné-Loccoz, M. A. Siegler, D. P. Goldberg, *J. Am. Chem. Soc.* **2013**, *135*, 10590–10593.
- [20] a) R. Latifi, M. A. Sainna, E. V. Rybak-Akimova, S. P. de Visser, *Chem. Eur. J.* **2013**, *19*, 4058–4068; b) S. M. Pratter, C. Konstantinovics, C. L. M. DiGiuro, E. Leitner, D. Kumar, S. P. de Visser, G. Grogan, G. D. Straganz, *Angew. Chem.* **2013**, *125*, 9859–9863; *Angew. Chem. Int. Ed.* **2013**, *52*, 9677–9681.
- [21] a) J. M. Mayer, *Acc. Chem. Res.* **1998**, *31*, 441–450; b) J. Yoon, S. A. Wilson, Y. K. Jang, M. S. Seo, K. Nehru, B. Hedman, K. O. Hodgson, E. Bill, E. I. Solomon, W. Nam, *Angew. Chem.* **2009**, *121*, 1283–1286; *Angew. Chem. Int. Ed.* **2009**, *48*, 1257–1260; c) D. E. Lansky, D. P. Goldberg, *Inorg. Chem.* **2006**, *45*, 5119–5125.
- [22] a) S. P. de Visser, *J. Am. Chem. Soc.* **2006**, *128*, 9813–9824; b) D. Kumar, W. Thiel, S. P. de Visser, *J. Am. Chem. Soc.* **2011**, *133*, 3869–3882.
- [23] A. K. Vardhaman, C. V. Sastri, D. Kumar, S. P. de Visser, *Chem. Commun.* **2011**, 47, 11044–11046.